JOURNAL OF MATERIALS SCIENCE 18 (1983) 2393–2400

Strength and fracture of amorphous and partially crystallized selenium

A. R. DAUDI*, K. N. SUBRAMANIAN
Department of Metallurgy, Mechanics and Materials Science, Michigan State University, East Lansing, MI 48824, USA

The role of spherulitic crystallization on strength and fracture of the elemental glass-former selenium was investigated. Partially crystallized selenium samples having various sizes and volume fractions of spherulites were obtained by heat-treating amorphous selenium at 62, 82 and 100° C for different lengths of time. The flexure strength of partially crystallized selenium decreases with increasing size of spherulites. Scanning electron microscopy of fractured specimens showed that fracture nucleated in the peripheral regions of the spherulites.

1. Introduction

Extensive investigations of the mechanical properties and fracture surface analysis of glass–crystal composites have been carried out with oxide–glass matrices [1–15]. In these studies, the crystalline phases have been obtained by heat-treatment, or have been purposely incorporated during fabrication [9]. The spherulite crystals obtained during the heat-treatment of amorphous selenium are spherical in shape: furthermore, the chemical composition of the crystal is the same as that of the amorphous matrix. These considerations make partially-crystallized selenium an ideal model for investigations of the mechanical behaviour of glass–crystal composites. A study dealing with strength of amorphous selenium suggests that the properties of amorphous selenium are comparable to amorphous polymers having similar structures [16], rather than to silicate glasses that have a network structure.

The purpose of the present investigation is to study the role of spherulitic crystallization on the mechanical properties of the elemental glass-former selenium, which does not have a three-dimensional network structure.

2. Experimental procedure

Bulk amorphous selenium samples were obtained by melting approximately 300 g of selenium in evacuated quartz ampoules in a rotary tube furnace, and by quenching the ampoules in ice-water bath. The melting procedure used to obtain amorphous selenium consisted of three distinct steps.

In the first step, selenium was melted in quartz tubes and rotated in a horizontal position for 24 h at 300° C. In the second step the furnace was made vertical and the temperature was raised to 600° C. The melt was held at this temperature for four hours to drive locked vapours out of the melt in order to produce pore-free samples. In the third step the furnace temperature was reduced to 300° C and the melt was held at this temperature for 20 h before quenching in an ice-water bath, so as to reduce the length of the pipe in the solid specimen. Further, the last step was essential to obtain glass specimens with reproducible properties. All these steps were carried out with remote control so as to minimize direct physical contact with poisonous selenium.

Test specimens (6.4 mm x 51 mm x 38 mm) were cut from the amorphous samples with a high precision diamond saw. After polishing by standard metallographic techniques, specimens were heat-treated at 100° C, 82° C and 62° C for different lengths of time to obtain various sizes and volume fractions of crystallites. The heat-treated specimens were ground to remove about 0.5 mm

*Present address: Motor Wheel Corporation, Lansing, MI 48909, USA

0022–2461/83 $03.00 + .12

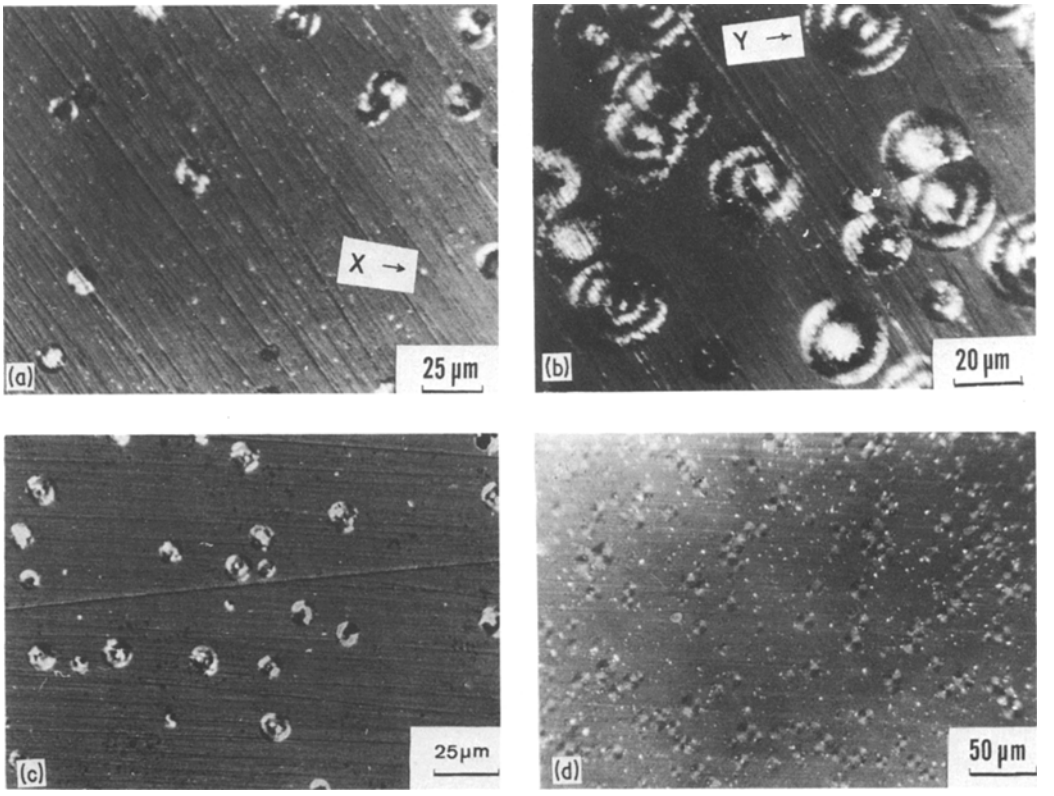

Figure 1 Typical microstructures of specimens heat-treated for (a) 1 hour at 100° C (b) 1 1/2 hours at 100° C (c) 6 hours at 82° C and (d) 311 hours at 62° C. [X and Y indicate monoclinic and trigonal (spherulite) crystals].

from each surface to eliminate surface undulations and the effects of surface crystallization. These specimens were polished by metallographic techniques to obtain a mirror finish. The volume fractions of crystallites were determined by point-count method with a polarized light microscope. The room temperature flexure strength, σ, was determined by three-point bending test in an Instron testing machine with a cross-head speed of 0.005 cm min^{-1} and with 25 mm and 12.5 mm spans. Twenty-seven specimens were tested to obtain the data point for each crystal size and volume fraction studied. The fracture surface energy, γ, was determined by breaking notched bars in three-point bending using the method of Davidge and Tappin [17] and the equation by Irwin and Orowan [18]. From the experimentally obtained σ, γ and E, the flaw size was determined.

The fracture surfaces were examined by scanning electron microscopy to obtain information about fracture origin, and other features.

3. Results and discussion

Typical microstructures of specimens heat-treated at various temperatures are shown in Fig. 1. A relatively small volume fraction of the crystalline phase is monoclinic selenium [marked X in Fig. 1a], and a large fraction is spherulitic selenium [marked Y in Fig. 1b]. Since the size and volume fraction of monoclinic selenium was very small throughout this investigation, results are analysed on the basis of spherulitic selenium only.

A plot of flexure strength as a function of volume fraction of spherulites is given in Fig. 2. This plot does not differentiate on the basis of the size of the spherulites. It illustrates that the decrease in flexure strength is much more drastic at low volume fractions [Fig. 2a] than at high volume fractions [Fig. 2c]. In order to understand the effect of volume fraction of spherulites, the flexure strength is plotted in Fig. 3 as a function of volume fraction for different sizes of spherulites. The selected spherulite diameters are 12.6, 15.8, 19.0, 22.2, 25.1 and 50.8 μm. Flexure strength decreases slightly with increase in volume fraction of small spherulites (12.6 μm) as shown in Fig. 3a. As the size of the spherulites becomes larger, their volume fraction has no effect on the

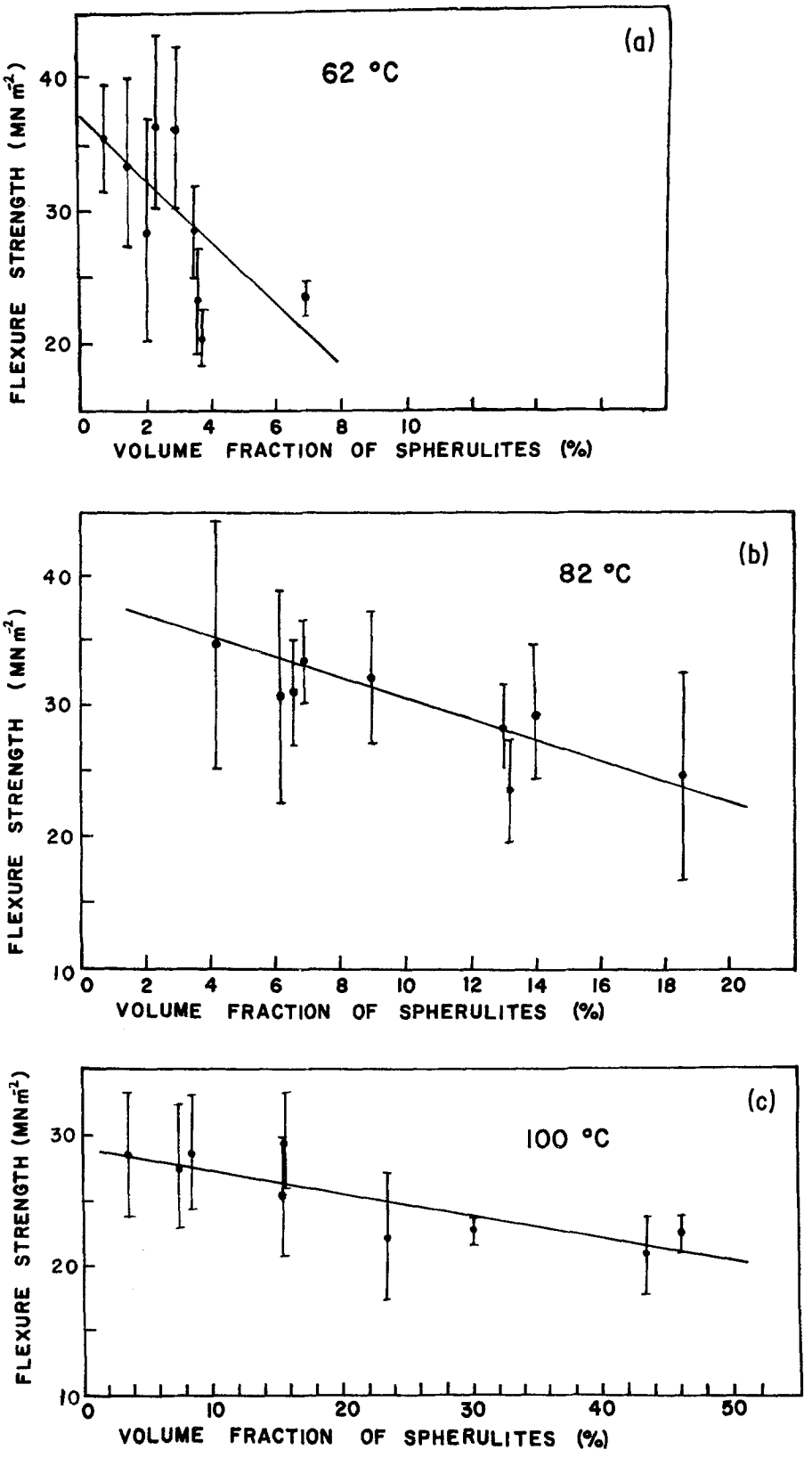

Figure 2 Flexure strength of partially crystallized selenium heat-treated at (a) 62° C (b) 82° C and (c) 100° C.

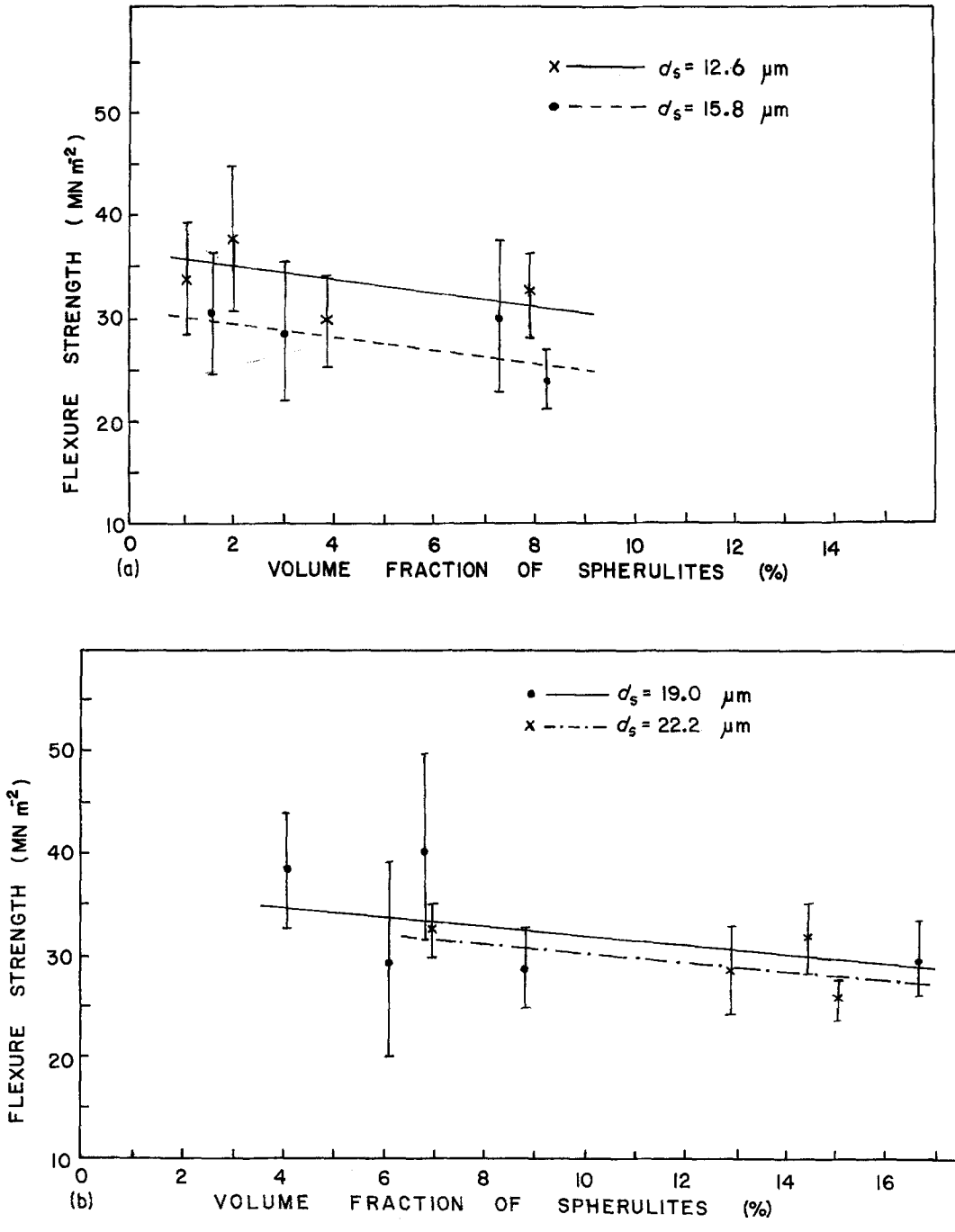

Figure 3 Flexure strength of partially crystallized selenium containing spherulites of diameter (a) 12.6 μm and 15.8 μm, (b) 19.0 μm and 22.2. μm and (c) 25.1 μm and 50.8 μm.

strength as shown in Fig. 3b and c. The fracture surface energy of amorphous selenium ($\gamma = 1.63 \times 10^{-3}$ J m^{-2}) decreases by a very small amount for partially crystallized selenium having a spherulitic volume fraction of approximately 50% ($\gamma = 1.50 \times 10^{-3}$ J m^{-2}). Since these values are so close, an average of these two values ($\gamma = 1.565$ J m^{-2}) was used to analyse the results during this investigation. Fractographs of amorphous and partially crystallized selenium are presented in Fig. 4. The three regions of fracture, (i) origin, (ii) mirror, and (iii) a frosty band that forms the boundary of the mirror area which usually becomes more hackled with increasing distance from the origin of fracture

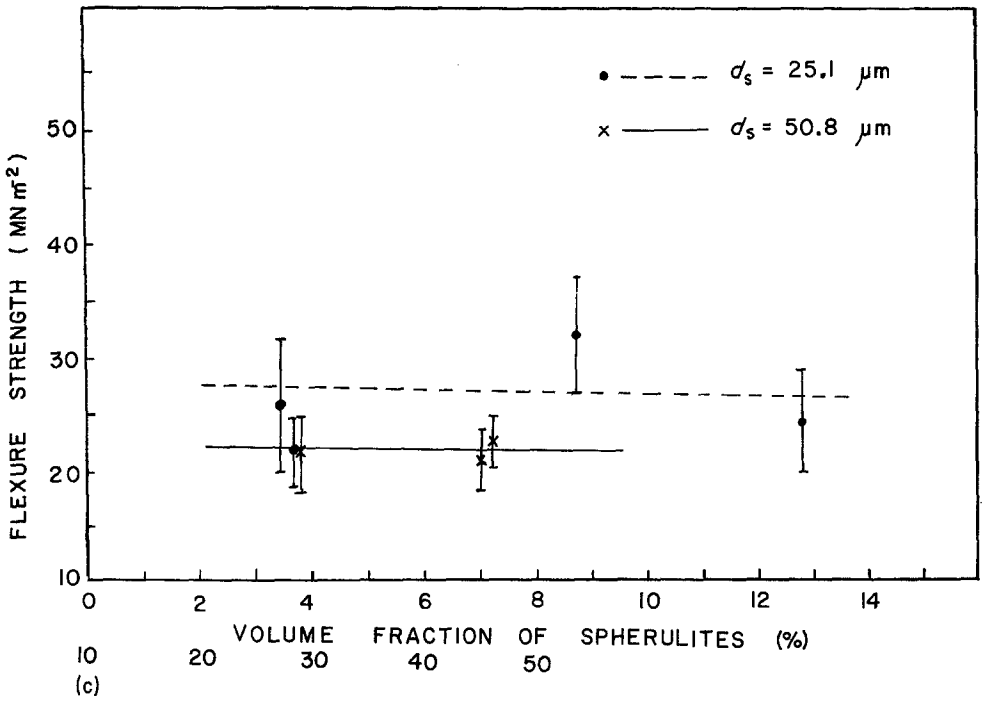

Figure 3 Continued

can be clearly seen in these fractographs. With an increased volume fraction of crystallites, the fracture tends to extend the mirror region.

The fracture origins in two partially crystallized specimens are presented in Figs. 5a and b. As can be seen in these micrographs, the presence of the spherulites in the mirror and hackle regions of fracture produces trail-like appearance as shown in Figs. 6a and b, respectively. Sometimes under very rare circumstances, the spherulite is pulled out of the fracture surface leaving a pocket as shown in Fig. 7. Details in the fractured spherulites are presented in Fig. 8. As can be seen from these scanning electron micrographs, the fracture path is somewhere in the periphery of the spherulite. The core of the spherulite is intact, and the glass–crystal interface shows no separation. This observation strongly suggests that the weakest region in the spherulite is the peripheral region. The inner core of these crystals, which is approximately half the diameter of the spherulite in large spherulites, tends to be dense and compact. In such specimens the fracture path tends to follow a region outside the inner core. In small spherulites the fracture path is very near the glass–crystal interface, indicating that the crystal is almost fully dense and compact.

Various investigators, for example, Frey and Mackenzie [6], and Binns [7], have attributed the decrease in flexure strength of glass–crystal composites to internal stresses due to the difference in thermal expansion of the glass and crystalline phases. These stresses could cause cracking in the matrix or the glass–crystal interface. According to Selsing [19], for a spherical inclusion, the radial and the tangential stresses will be directly proportional to the difference in the coefficients of thermal expansion. However, the thermal expansion coefficient of spherulitic selenium (trigonal selenium) is $37.79 \times 10^{-6}\,^{\circ}C^{-1}$ and that of amorphous selenium is $37.73 \times 10^{-6}\,^{\circ}C^{-1}$. These two values are so close, and as a result only a small radial tensile stress would exist at the glass–crystal interface, and if failure occurs, the crack will have to propagate circumferentially around the spherulite. Even if we consider that spherulites to be made up of lamella of trigonal selenium arranged annularly, as suggested by Fitton and Griffiths [20], the resultant increase in coefficient of thermal expansion in the radial direction would increase the radial tensile stress and would result in a circumferential cracking at the glass–crystal interface. Throughout this investigation there was no evidence of cracking in the glassy matrix or at the glass–crystal interface. It can be concluded that premature cracks caused by internal stresses do not exist in partially crystallized selenium.

Stress concentration due to the presence of

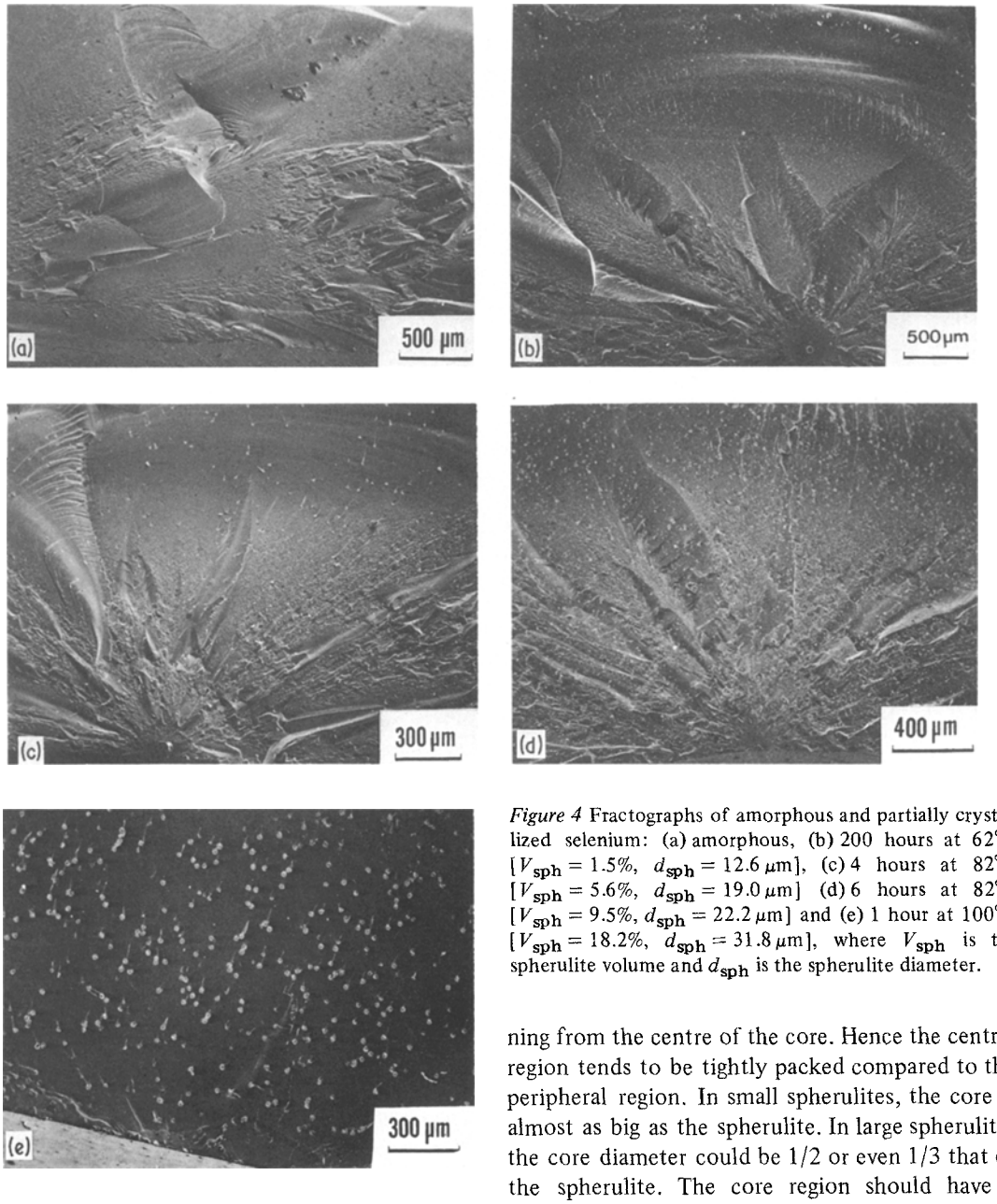

Figure 4 Fractographs of amorphous and partially crystallized selenium: (a) amorphous, (b) 200 hours at 62° C [$V_{sph} = 1.5\%$, $d_{sph} = 12.6\,\mu m$], (c) 4 hours at 82° C [$V_{sph} = 5.6\%$, $d_{sph} = 19.0\,\mu m$] (d) 6 hours at 82° C [$V_{sph} = 9.5\%$, $d_{sph} = 22.2\,\mu m$] and (e) 1 hour at 100° C [$V_{sph} = 18.2\%$, $d_{sph} = 31.8\,\mu m$], where V_{sph} is the spherulite volume and d_{sph} is the spherulite diameter.

spherical inclusions could be another possibility [8, 9]. It should be noted that the peripheral region of spherulites is also the region of stress concentration. The glass–crystal interface seems to be stronger than the spherulite itself since cracks have never been observed at the interface.

Spherulite, when observed at high magnification, exhibits two distinct regions: The central region, which may be called the core, and an outer region, can be observed in Figs. 8a and b. Lamella of trigonal selenium are arranged as spirals beginning from the centre of the core. Hence the central region tends to be tightly packed compared to the peripheral region. In small spherulites, the core is almost as big as the spherulite. In large spherulites the core diameter could be 1/2 or even 1/3 that of the spherulite. The core region should have a higher Young's modulus compared to peripheral region due to its tighter packing.

In partially crystallized selenium samples studied in this investigation, the crystalline phase was the discontinuous phase and the glassy phase was the continuous phase. In glass–crystal composites containing a hard crystalline phase, the distributed crystalline phase tends to restrict the flaw size in the glassy matrix, and the flexure strength is controlled by the inter-particle (crystal) spacing, which will be the mean free path [2]. The flaw size (40 μm) calculated from the fracture

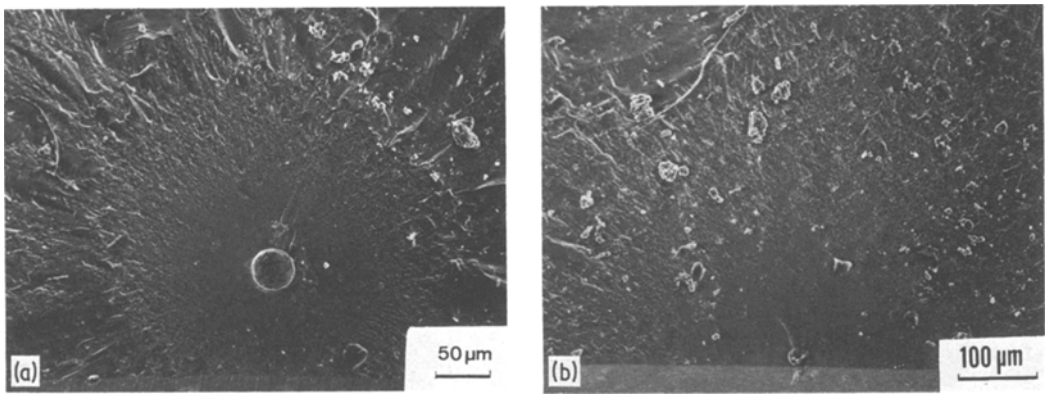

Figure 5 Fractograph of partially crystallized selenium showing (a) internal origin at a spherulite, (b) near-surface origin at a spherulite. The specimen surface can be seen at the lower edge of these micrographs.

strength for a low volume fraction (2%) of small spherulites (15.8 μm) is very much smaller than the calculated mean free path (743 μm). At higher volume fraction (46%) and with large spherulites (50.8 μm), the calculated mean freee path (59.6 μm) is smaller than the flaw size (90.5 μm). The flexure strength is found to be relatively insensitive to change in the volume fraction of spherulites. It is, therefore, possible to conclude that the glassy phase present in partially crystallized selenium does not contain the flaws or the microcracks that result in decrease of its flexure strength. The flaws have to be present in the crystalline phase or the glass–crystal interface. Utsumi and Sakka [21] have suggested that under such conditions mechanical strength, σ, is dependent on mean crystal diameter, d, according to the relationship

$$\sigma = kd^{-1/2} \quad (1)$$

where k is a constant. This relationship implies that the crack length is proportional to or equal to the crystal diameter. Detailed analysis of test results of partially crystallized selenium indicates that the calculated flaw size is usually 1.0 to 3.0 times the diameter of the spherulite (the larger value corresponding to smaller size crystals). This suggests that the flaw lies in the peripheral regions of the spherulite. Such flaws can be seen in Fig. 8. A schematic diagram of the flaw geometry is given in Fig. 8c. This flaw has a size larger than the diameter of the spherulite although it cannot provide a flaw size to crystal diameter ratio as high as three. These cracks may have developed as a result of drastic differences in elastic moduli between glassy and spherulitic crystalline selenium during stressing of the specimen, since the Young's modulus of amorphous selenium is 9.8×10^3 MN m^{-2} and that of trigonal (spherulitic) selenium is 57.9×10^3 MN m^{-2} [16, 22].

Conclusions

1. Selenium, an elemental glass former,

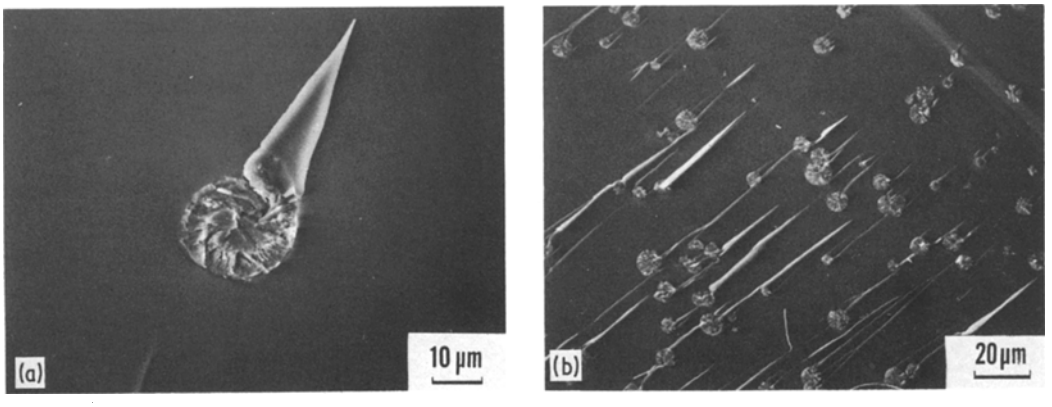

Figure 6 Trails produced by spherulites (a) in the mirror region (b) in the hackle region.

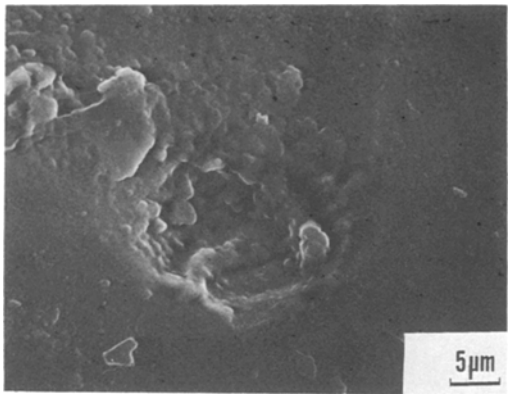

Figure 7 A pocket left by spherulite in mirror region.

becomes mechanically weak by spherulitic crystallization.

2. In partially crystallized selenium, the origin of fracture lies in the peripheral regions of spherulites.

3. The room temperature fracture behaviour of amorphous selenium having a polymeric structure is similar to that of glasses with a three-dimensional network structure. This similarity is not altered even under partially crystallized condition.

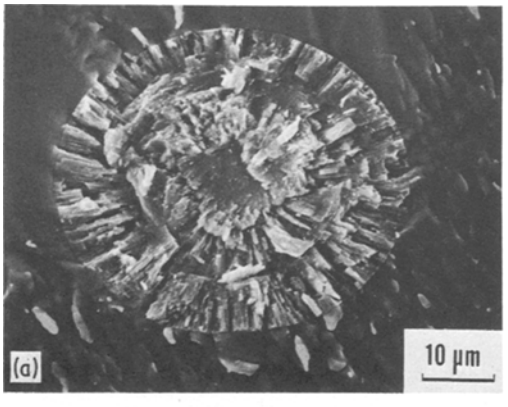

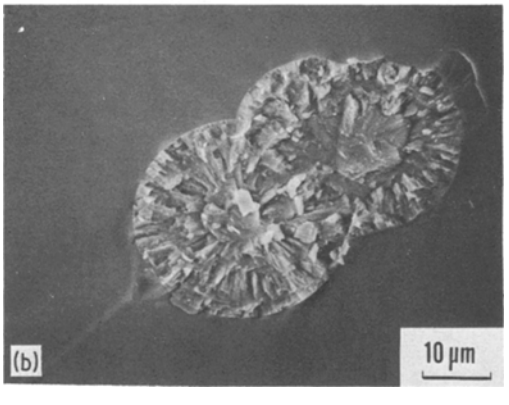

References

1. P. W. McMILLAN, S. V. PHILLIPS and G. J. PARTRIDGE, *J. Mater. Sci.*, **1** (1966) 269.
2. D. P. H. HASSELMAN and R. M. FULRATH, in "Ceramic Microstructures", edited by R. M. Fulrath and J. A. Park (Wiley, New York, 1968) p. 343.
3. S. W. FRIEMAN and L. L. HENCH, *J. Amer. Ceram. Soc.* **55** (1972) 86.
4. D. P. BISWAS and R. M. FULRATH, *ibid.* **58** (1975) 526.
5. M. P. BOROM, A. M. TURKALO and R. H. DOREMUS, *ibid.* **58** (1975) 385.
6. W. J. FREY and J. D. MACKENZIE, *J. Mater. Sci.* **2** (1967) 124.
7. D. B. BINNS in "Science of Ceramics" edited by G. H. Stewart (Academic Press, London, 1962) vol. 1, p. 315.
8. D. P. H. HASSELMAN and R. M. FULRATH, *J. Amer. Ceram. Soc.* **48** (1965) 218.
9. *Idem, ibid.* **48** (1965) 218.
10. *Idem, ibid.* **50** (1967) 399.
11. G. K. BANSAL and W. H. DUCKWORTH, *ibid.* **60** (1977) 304.
12. H. P. KIRCHNER, R. M. GRUVER and W. A. SOTTER, *Mater. Sci. Eng.* **22** (1976) 147.
13. J. J. MECHOLSKY, S. W. FRIEMAN and R. W. RICE, *J. Mater. Sci.* **11** (1976) 1310.
14. J. J. MECHOLSKY, R. W. RICE and S. W. FRIEMAN, *J. Amer. Ceram. Soc.* **57** (1974) 440.
15. J. J. MECHOLSKY, S. W. FRIEMAN and R. W. RICE, *ibid.* **60** (1977) 114.
16. D. LEWIS III, W. C. LACOURSE and D. B. HARDY, *ibid.* **60** (1977) 107.
17. R. W. DAVIDGE and G. TAPPIN, *J. Mater. Sci.* **3** (1968) 165.
18. E. OROWAN, *J. Welding* **34** (1955) 157.
19. J. SELSING, *J. Amer. Ceram Soc.* **44** (1961) 419.
20. B. FITTON and C. A. GRIFFITHS, *J. Appl. Phys.* **39** (1968) 3663.
21. Y. UTSUMI and S. SAKKA, *J. Amer. Ceram. Soc.* **53** (1970) 286.
22. D. SNELL and L. S. ETTRE, *Encyclopedia Ind. Chem. Anal.*, **17** (1973) 583.

Received 22 November 1982
and accepted 5 January 1983.

Figure 8 Details in fractured spherulites showing (a) core and peripheral regions in a single spherulite, (b) core and peripheral regions in overlapping spherulites and (c) schematic of the flaw.